Friction **11**(8): 1534–1543 (2023)
https://doi.org/10.1007/s40544-022-0715-5
ISSN 2223-7690
CN 10-1237/TH
RESEARCH ARTICLE

Rubber–ice friction

Toshi TADA[1], **Satoshi KAWASAKI**[1], **Ryouske SHIMIZU**[1], **Bo N. J. PERSSON**[2,3,*]

[1] *Sumitomo Rubber Industries, Ltd., Material Research & Development HQ. 2-1-1, Kobe 651-0071, Japan*

[2] *Peter Grünberg Institute (PGI-1), Forschungszentrum Jülich, Jülich 52425, Germany*

[3] *MultiscaleConsulting, Jülich 52428, Germany*

Received: 04 August 2022 / Revised: 12 October 2022 / Accepted: 26 October 2022

Abstract: We study the friction when a rectangular tire tread rubber block is sliding on an ice surface at different temperatures ranging from −38 to −2 °C, and sliding speeds ranging from 3 μm/s to 1 cm/s. At low temperatures and low sliding speeds we propose that an important contribution to the friction force is due to slip between the ice surface and ice fragments attached to the rubber surface. At temperatures above −10 °C or for high enough sliding speeds, a thin premelted water film occurs on the ice surface and the contribution to the friction from shearing the area of real contact is small. In this case the dominant contribution to the friction force comes from viscoelastic deformations of the rubber by the ice asperities. We comment on the role of waxing on the friction between skis and snow (ice particles).

Keywords: ice friction; rubber friction; ice premelting

1 Introduction

Friction on ice is a fascinating topic with a long history [1–5]. Pioneering work was done by Faraday [6] more than 150 years ago. He brought two ice cubes into contact and found that they instantly froze together. He concluded that the surface of ice is covered by a liquidlike water layer, but a recent study suggest a different explanation namely sintering caused by sublimation and condensation [7]. Thomson [8] suggested that the liquid-like layer is due to pressure melting. Pressure melting was often used as an explanation for the low friction on ice for the following 40 years, until Bowden and Hughes [9] suggested that frictional heating might result in melting of the ice surface, and that this is the main reason for the low friction of ice at enough high sliding speed.

Many crystalline solids exhibit surface premelting, where a liquidlike layer forms at the surface before the whole body melts [10–13]. In the simplest picture this can be explained by the fact that the atoms or molecules at the surface of a solid are bound to less number of neighbors than those in the bulk and will break loose because of thermal fluctuations before the whole crystal melt. The low friction of ice can be attributed to a combination of frictional heating and ice premelting. However, while many experiments have shown that the free ice–vapor interface undergoes premelting, starting at least 10 °C below the bulk melting temperature [14–16], there are almost no experimental studies showing that the same is true at the interface between ice and another solid [17]. Thus, most of the experimental technique used to study the ice–vapor interface cannot be used to study the (buried) interface between ice and another solid.

It depends on the chemical nature of the solid if a liquid-like water film can form between ice and another solid [18]. Thus, for very inert (hydrophobic) materials such as polytetrafluorethylene (Teflon) or polyethylene in contact with ice, a premelted layer may occur below the ice melting temperature. For solids with strong water–solid interaction, such as (hydrophilic) silica,

* Corresponding author: Bo N. J. PERSSON, E-mail: b.persson@fz-juelich.de

or some metal oxides, the liquidlike layer may not occur, or may occur only in a narrower temperature interval close to the ice melting temperature. However, there are experimental results indicating that a liquidlike layer may occur below the bulk melting temperature even for ice in contact with ice if the two crystal lattices are incommensurate oriented (e.g., rotated). This is also consistent with the fact that many crystalline solids start to melt at grain boundaries before the whole material melts [19, 20]. Still, the frictional shear properties of this liquidlike layer may be very different from that occurring at the interface between, e.g., Teflon and ice.

Here we note that two recent studies have proposed very different origins of the friction on ice. Reference [21] showed the importance of the ploughing contribution, while in Ref. [22] it was found that during reciprocated sliding on ice a lubricating, viscous mixture of liquid water and ice particles dominates the frictional behavior.

Another recent study addressed ice speed skating. In Ref. [23] it was shown that the friction between the steel skate blade and the ice stems from boundary friction, where the temperature of the interface is below zero and ice surface molecules exhibit unconventional mobility, and hydrodynamic friction where the ice melts and a thin water layer between the blade and the ice forms. The boundary friction only plays a role at the tip of the skate blade over an extremely short contact length between the skate blade and the ice, and gives a negligible contribution to total friction but generates enough heat to melt the ice which allows the skater to slide smoothly on a thin layer of melt water.

In this paper, we study the friction between rubber and ice. Rubber friction on ice has many applications, and is particularly important for understanding the grip of tires on icy road surfaces [24–29]. We will show that for very low temperatures (T < −15 °C) rubber friction on ice gives a velocity and temperature-dependent friction coefficient very similar to those of ice sliding on ice. We interpret this as due to the slip between the ice surface and ice fragments attached to the rubber surface. For T > −10 °C, the rubber–ice friction differs drastically from the ice–ice friction which we attribute to two effects, namely the formation of a premelted water film and slip at the rubber–ice interface, and to a viscoelastic contribution to the friction from the deformations of the rubber surface by the ice asperities.

In general, for sliding speeds above ~0.1–1 m/s the frictional heating is high enough to melt a thin ice layer and the friction is determined mainly by fluid dynamics at an interface with a complex gap (surface separation) determined by the surface roughness. In this paper we will focus on low sliding speeds ($v \le 1$ cm/s) where the ice does not melt but where ice premelting may result in a thin liquidlike film which strongly reduce the sliding friction force. We note that the nature of the friction force for low sliding speeds is very important for tire dynamics as it determines the effective static friction force, and hence the line separating the region where the tread blocks are not sliding (or slide at very low speeds of $v < 1$ mm/s), from the region where they slide (typical slip velocity ≈ 1 m/s).

2 Experimental

2.1 Low-temperature friction tester

We have performed ice friction measurements using our low-temperature linear friction slider. In this set-up the temperature can be changed from room temperature down to −40 °C. The rubber is glued on the sample holder (aluminum plate) (Fig. 1) which gets attached to the force cell. The rubber specimen can move with the carriage in the vertical direction to adapt to the substrate profile. The normal load can be changed by adding steel plates on top of the force cell. The substrate sample gets attached to the machine

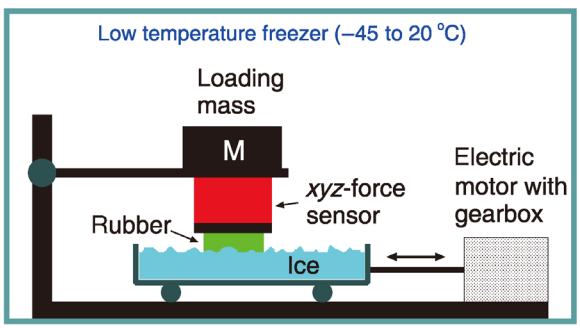

Fig. 1 Schematic picture of low-temperature friction instrument allowing for linear reciprocal motion.

table which is moved by a servo drive via a gearbox in a translational manner. We control the relative velocity between the rubber specimen and the substrate sample while the force cell acquires information about normal force as well as the friction force.

To change the temperature, and to avoid (or reduce) the condensation of moisture in the atmosphere on the rubber and ice surfaces, the whole set-up is placed inside a deep freezer. We slide the rubber sample over the ice surface with various velocities to gain information on the velocity and temperature dependence of the friction coefficient. With the current configuration it is possible to move the rubber specimen with velocities from 1 μm/s to 12.5 mm/s. For increasing the temperature after an experiment is finished there is a heating system built into the set-up.

2.2 Ice surface

The ice surface was produced according to the procedure I1 described in Ref. [27]. Thus, distilled water was poured into an aluminum box and frozen to make a thin ice layer. The thin ice layer was created repeatedly to obtain a thick ice substrate without (or with reduced) surface unevenness resulting from freezing-induced expansion of water (note: Ice has a bigger volume than water at 0 °C). In Ref. [27] it was shown that the surface roughness power spectrum of the ice surface prepared this way is very similar to the power spectra obtained from ice surfaces produced using other different procedures. We have not studied the surface topography of the ice surface used in the present study but we assume that it is similar to that of the ice surface I1 studied in Ref. [27].

The red line in Fig. 2 shows the surface roughness power spectrum of the ice surface used in the viscoelastic friction calculations. The blue lines are the power spectrum of the rubber surface obtained from stylus line scans performed at different locations on the rubber block. The power spectrum of the ice surface is much larger than that of the rubber surface and we can neglect the surface roughness on the rubber block. In general, roughness on the rubber surface affects the area of real contact and the adhesive contribution to the friction. However, during steady sliding at a constant speed on a smooth counter surface there is no viscoelastic contribution to the friction from the rubber asperities as there is no time dependent deformations of the rubber.

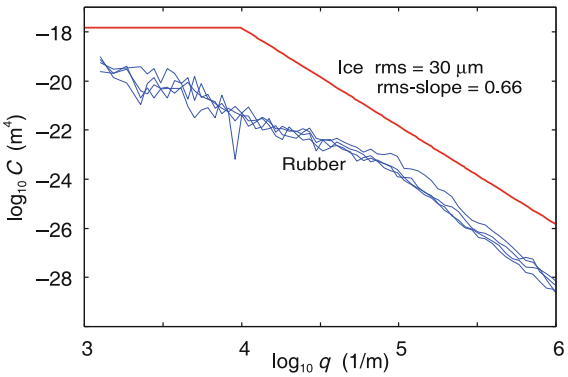

Fig. 2 Red line is the surface roughness power spectrum of the ice surface used in the viscoelastic friction calculations. Blue lines are the power spectrum of the rubber surface obtained from stylus line scans performed at different locations on the rubber block.

2.3 Rubber compound

In the present study we use a rubber compound consisting of a blend of natural rubber, butadiene rubber and styrene–butadiene rubber with silica filler. This is a winter tread compound with the glass transition temperature of $T_g \approx -45$ °C. The rubber block is 1 cm thick, 6 cm wide and 2 cm long in the sliding direction.

The viscoelastic modulus of the rubber was measured using dynamical mechanical analysis (DMA) with DMA+450 (Metravib). The dynamic moduli is obtained for a fixed stress amplitude using the standard frequency–temperature shifting procedure, where the frequency range between 0.1 and 100 Hz and the temperature varied in the range of −50 to 80 °C. Plane shear geometry is employed to apply shear deformation to two disc shaped-samples, the height and diameter of the discs are 1 and 10 mm, respectively. The dynamic strain amplitude was 0.1% at low temperatures near T_g but increases so that the force range is in the reliable value at higher temperatures.

Figure 3 shows the logarithm of the real part of the viscoelastic modulus, and the ratio ImE/ReE between the imaginary and the real part of the viscoelastic modulus, as a function of the logarithm of the frequency.

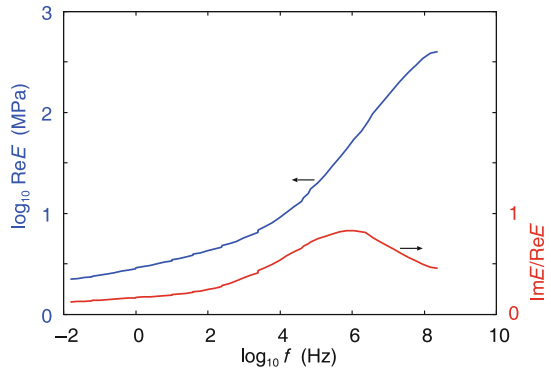

Fig. 3 Logarithm of the real part of the viscoelastic modulus, and ImE/ReE as a function of the logarithm of the frequency (f). The reference temperature is T = 20 °C.

3 Experimental results

We present experimental friction results for the nominal rubber–ice contact pressure of p_0 = 0.2 MPa, as typical for tire applications. The temperature inside the deep freezer is varied in steps from −38 to −2 °C. We start at the lowest temperature and for each temperature we increase the sliding speed in steps, from 3 μm/s up to 1 cm/s. For the two lowest sliding speeds (3 and 10 μm/s) we slide 2 cm on the ice surface and for the six highest speeds (30, 100, and 300 μm/s; 1, 3, and 10 mm/s) we slide 4 cm so total 28 cm sliding distance. The friction coefficients reported below are averages of F_x/F_z over the sliding distance (2 or 4 cm) for each velocity.

Figure 4 shows the measured rubber–ice friction coefficient as a function of the logarithm of the sliding speed for several temperatures indicated. For each temperature we slide on the same ice surface track. Thus, the first data (at −38 °C) may be influenced by run-in of the ice surface where some of the ice asperities are smoothed by plastic deformation and wear.

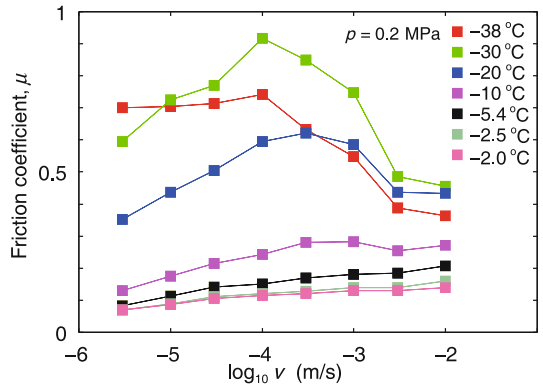

Fig. 4 Measured rubber–ice friction coefficient as a function of the logarithm of the sliding speed (v) for several temperatures indicated. The nominal contact pressure is p = 0.2 MPa.

4 Analysis of experimental data and discussion

There are two contributions to the rubber friction on ice, namely a contribution from shearing the area of real contact and a contribution from the viscoelastic deformations of the rubber surface by the ice asperities. In Ref. [27] we studied the viscoelastic contribution (μ_{visc}) to the friction, and we will use the same theory in the present case (also in Ref. [30]). The calculations of μ_{visc} enter the viscoelastic modulus $E(\omega)$ of the rubber compound, and the ice surface roughness power spectrum $C(q)$. We assume that the latter is similar to that of the ice surface I1 studied in Ref. [27]; the power spectra used in the calculations below are given by the red line in Fig. 2. In Ref. [27] the large wavenumber cut-off q_1, which determines the shortest wavelength roughness included when calculating μ_{visc}, was determined so that the rubber–ice maximum contact stress is given by the plastic yield properties of the ice. However, in the present case, including the roughness over all the length scales studied in Ref. [27] ($q < 10^6$ m^{-1}), results in contact stresses (see Fig. 5) below the ice penetration hardness (which depends on the temperature and the indentation speed). In what follows we use $q_1 = 10^6$ m^{-1} for all temperatures and sliding speeds. The exact origin and magnitude of the cut-off q_1 in the present case is not

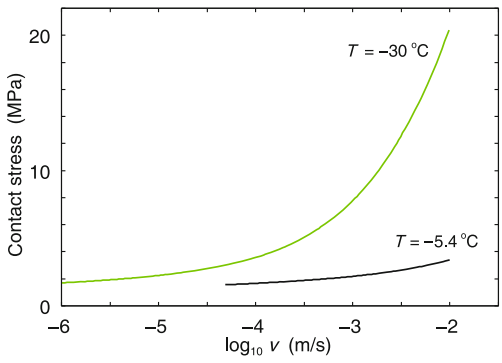

Fig. 5 Calculated contact stress as a function of the logarithm of the sliding speed (v) for T = −30 and −5.4 °C assuming that the rubber is sliding on a rigid surface with the power spectrum shown by the red line in Fig. 2.

known to us but using a larger wavenumber cut-off would result in a friction coefficient (for the largest sliding speed) which is larger than observed.

In Fig. 6 we show the measured friction coefficient as a function of the logarithm of the sliding speed at T = −30 and −5.4 °C (from Fig. 4), and the calculated viscoelastic contribution (solid lines) for the same temperatures①. The rubber viscoelastic modulus was not measured to low enough frequencies to obtain the friction for T = −5.4 °C for the three lowest experimental velocity data points. Figure 6 shows that for T = −5.4 °C the viscoelastic contribution alone gives nearly the full experimentally measured friction, i.e., the contribution from the area of real contact must be very small. This is the expected result if a thin premelted liquidlike water film occurs in the area of real contact. At T = −30 °C the viscoelastic contribution can explain the measured data only for the highest sliding speed. At high sliding speeds, frictional heating is important which may result in a premelted surface layer which gives a negligible contribution to the friction. However, for low sliding speeds the measured friction is much larger than the viscoelastic contribution. This implies that there must be a contribution from the area of real contact, and that no liquidlike film occurs in the rubber–ice contact

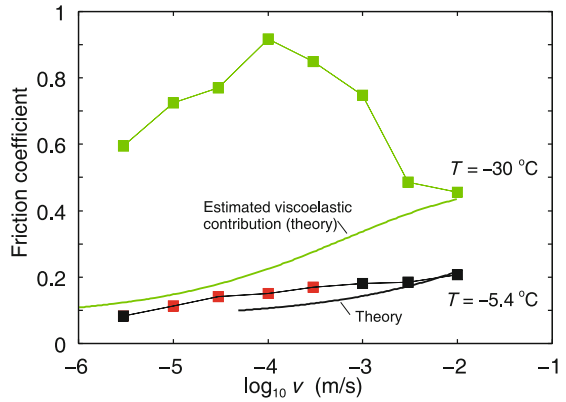

Fig. 6 Measured friction coefficient as a function of the logarithm of the sliding speed (v) for T = −30 and −5.4 °C (from Fig. 4) and the calculated viscoelastic contribution (solid lines) for the same temperatures. The nominal contact pressure is p = 0.2 MPa.

① In Ref. [31] the theory presented in Ref. [32] and used above was compared to (viscoelastic) boundary element calculations, and it was found that the theory may overestimate the viscoelastic contribution at high velocities, where the contact area is small. However, similar simulations presented in Ref. [30] gave results in good agreement with the theory for all sliding speeds.

regions in this case. We will now discuss the physical origin of the area of real contact contribution to the friction force for low temperatures and low sliding speeds.

Figure 7 shows the measured ice–ice friction coefficient as a function of the sliding speed for several temperatures indicated. Note that at T = −40 and −30 °C at low sliding speeds the magnitude and velocity dependence of the ice–ice friction coefficient is very similar to what we observe for the rubber–ice friction. Hence, we propose that for low temperatures ice fragments attach to the rubber surface and that the slip occurs at the interface between the ice fragments and the ice surface. These ice fragments may result from ice wear processes or from frost crystals formed on the rubber and ice surfaces before start of sliding. We note that in our low-temperature set-up we first

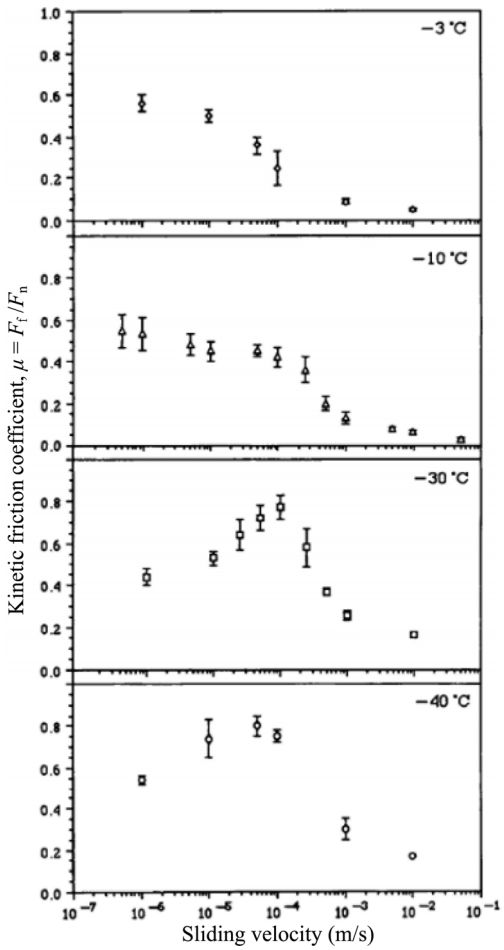

Fig. 7 Measured ice–ice friction coefficient as a function of the sliding speed for several temperatures indicated. The nominal contact pressure is p = 0.02 MPa. Reproduced with permission from Ref. [33], © Taylor & Francis Ltd 2000.

cool down the system to −40 °C (which takes several hours) without the rubber in contact with the ice. After we open the deep freeze and lower the rubber to the ice surface. This act takes ~10 s and may result in humid air flowing to the ice and rubber surfaces where it could form loosely bound ice structures (frost). This is also consistent with observations of Roberts [24] who found that rubber friction on frosty ice is much smaller than that on polished ice. He found that the friction coefficient on polished ice at v = 10 mm/s was about ~1.8 but only ~0.5 on the same ice covered with hoar frost, which is similar to what we observe when v = 10 mm/s and T < −20 °C. He also observed that at −30 °C a polished ice track would remain so only for a few hours, despite being in a closed deep freeze cabinet. This may be a result of ice sublimation and formation of small frost crystals, and is likely to occur in our experimental set-up, too.

At T > −10 °C the magnitude and the velocity dependence are completely different for the ice–ice contact as compared to the ice–rubber contact. For the ice–ice contact, the friction decreases drastically with the increasing sliding speed. We have shown in Ref. [34] that this can be explained by premelting of the ice surface occurring as a result of frictional heating. However, at low sliding speeds, frictional heating is negligible and in this case even at T = −3 °C there is no premelted liquidlike film at the ice–ice interface and the sliding friction coefficient is very large (Fig. 7(top) for $v = 10^{-5}$ m/s). We propose that a premelted film occurs at the rubber–ice interface for any temperature above −10 °C, and that the observed sliding friction for these temperatures is mainly due to the viscoelastic contribution, which increases with the increasing sliding speed, as does the measured friction.

Direct observation of the influence of premelting at the rubber–ice contact for T > −10 °C was presented by Roberts [24] and Orndorf et al. [17], who observed very different types of adhesion between rubber balls and ice above and below ~−10 °C. In these studies it was also observed that after some minutes waiting time in lightly loaded static contact at T = −10 °C the rubber sphere made a circular mark in the ice indicating a continuous flow of water away from the contact during stationary contact. The same effect was not observed at T = −20 °C.

Experiments have shown that rubber may adhere strongly to smooth (polished) ice surfaces (as strong as to silica glass) and that the friction coefficient between rubber and polished ice surfaces may be very large (of order 2) for low sliding speeds and low temperatures (T < −10 °C, but $T > T_g$) [24, 25]. Thus, we expect that the velocity and temperature dependence of the rubber friction on ice will look qualitatively like that in Fig. 4 also when there are no ice fragments at the ice–rubber interface.

In order for ice fragments to be attached to the rubber surface and slide on the ice surface the ice–rubber friction must be larger than the ice–ice friction. This is supported by experimental data for smooth ice surfaces without frost crystals which show very high rubber friction (typically maximum around ~2). In addition, the friction we observe is of similar magnitude as the ice–ice friction (Figs. 4 and 7) so if our interpretation would be incorrect and the rubber would slide on the ice surface and then our result shows that the ice–rubber and ice–ice friction coefficients are of similar magnitude. So the ice–rubber friction cannot be smaller than the ice–ice friction.

Hemette et al. [35] have performed rubber–ice friction measurements on very smooth ice surfaces for temperatures between −20 and −2.5 °C. As a function of the logarithm of the sliding speed, they observed a Gaussian-like friction coefficient curve centered at $v \approx$ 10 mm/s with a maximum which decreased from ~2 at −20 °C to 0.2 at −2.5 °C. This differs from our study where the maximum of the friction at low temperatures is for $v \approx$ 0.1 mm/s. This difference is consistent with the assumption that in our study, the friction at low temperatures is due to ice sliding on ice while in the study of Hemette et al. [35] no frost crystals or ice wear particles occurred at the sliding interface.

Very different velocity and temperature dependence of the friction from what we found above have been observed for some non-rubber material sliding on ice. Thus, in Ref. [21] silicon carbide and steel balls was slid on ice. At the sliding speed of 0.38 mm/s and the temperature of T = −32 °C, the friction coefficient μ is about 0.1, to be compared to $\mu \approx$ 0.8 found in our study. For temperatures close to the ice melting temperature (T = −2 °C) we find $\mu \approx$ 0.15 while in

Ref. [21] the friction coefficient for a silicon carbide sphere first decreased to a very low value of ~0.02 at T = −8 °C, and then increased a lot on approaching the bulk ice melting temperature, which was interpreted in Ref. [21] as due to plowing. Clearly, the friction mechanism for rubber on ice must be very different from that for the systems studied in Ref. [21].

Finally, let us comment on ski–waxing. This is a very controversial topic and not well understood [36–39]. A related topic is the use of wax (and other hydrophobic coatings) on glass windows of cars to more easily remove rain drops [40, 41]. It is well known that on clean wet glass (which is hydrophilic) the rubber–glass friction is very low when the water film is thick enough as expected when the sliding speeds are high enough, but as the water film dries up the friction increases and reaches a maximum when a small amount (nanometer thickness) of water still remains on the glass surface [42]. This can be explained by capillary attraction which pulls the two surfaces together and increases the normal force and the friction [42–44] (note: Capillary attraction, due to the Laplace pressure, gets bigger, the thinner the water film). In addition the capillary bridges may "tilt" due to contact angle hysteresis which would contribute to a tangential (friction) force [39]. For a ski with a hydrophilic surface, such as a clean wood ski, the same effect could occur in some sliding velocity ranges where the water film is very thin.

On the wax-coated glass surface we expect smaller capillary adhesion friction than that for clean wood surface because the water contact angle is much larger on the wax-coated surface. At the high sliding speed in downhill skiing and also in cross country skiing (except when uphills) the sliding speed is so high as to generate a meltwater film at the ice–ski interface. However, because of the small size of ice particles (or snow flakes) the contact region between an ice particle and a ski is very small which favors quick removal of the melt water, and it may be that there will never be a thick water film in the ice–ski contact regions even at relative high sliding speeds. In this case for a strongly hydrophilic interface (as for clean wood skis) the capillary adhesion effect may be important and result in higher friction than that for the wax-coated wood skis where the capillary adhesion is much smaller.

For a rubber wiper blade on a wet wax-coated glass surface it is found that the friction for low sliding speeds is much higher than that for the clean wet glass surface [45, 46]. This is due to the fact that the water gets expelled from the rubber–glass contact area on the hydrophobic glass surface resulting in dry contact and high friction. We note that a just ~10 nm thick water film results in a very low viscous shear stress even at a relative high sliding speed like 1 m/s typically involved in wiper blade applications. While the wax-coated wood ski is hydrophobic (water contact angle is larger than 90°) the ice–wax interface is still hydrophilic (because of the low contact angle for water on ice), but the surface free energy reduction on forming capillary bridges is much smaller than that on the ice–wood interface, which will result in easier squeeze-out of the water film from the ice–wax interface. This higher friction expected for low sliding speeds for the wax-coated wood could be useful when moving uphill in cross country skiing. Also, for hydrophilic skis, snow could adhere to the skis during the uphill movement which would generate problems when entering a more horizontal or downhill part of the track.

5 Summary and conclusions

Figure 8 summarizes the proposed picture resulting from the study presented above. Figure 8(a) illustrates that when a rubber block is sliding on an ice surface for T > −10 °C a thin liquidlike film of premelted ice occurs at the interface between the rubber and the ice surface. Shearing the liquidlike film results in negligible contribution to the friction force which is hence mainly due to viscoelastic deformations of the rubber by the ice asperities.

However, at T < −15 °C and low enough sliding speeds, there is no premelted liquidlike film at the ice–rubber interface. In this case the friction force is mainly due to shearing of the contact area between the ice block and ice fragments adhering to the rubber surface (Fig. 8(b)), and to viscoelastic deformations of the rubber by the ice asperities. For temperatures below the T_g of the rubber the viscoelastic contribution will also be negligible.

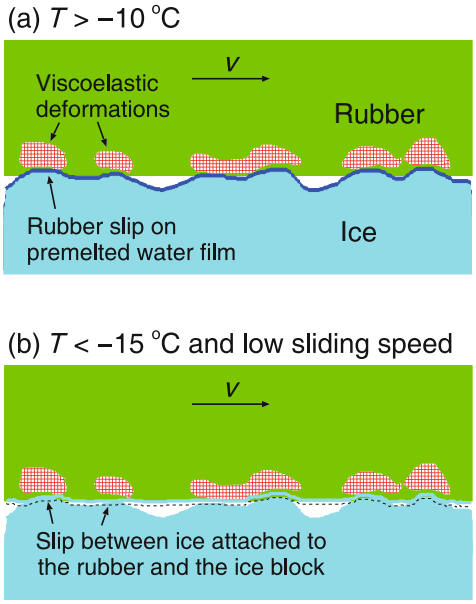

Fig. 8 (a) When a rubber block is sliding on an ice surface for $T > -10$ °C a thin liquidlike film of premelted ice occurs at the interface between the rubber and the ice surface. (b) For $T < -15$ °C there is no premelted liquidlike film at the ice–rubber interface, but we propose that ice fragments adhering to the rubber surface and that slip occur between the ice fragments and the ice surface.

Acknowledgements

We thank A. ALMQVIST and R. LARSSON (Luleå Technical University, Sweden) for comments on the text and for useful discussions.

References

[1] Rosenberg R. Why is ice slippery? *Phys Today* **58**(12): 50–55 (2005)

[2] Kietzig A M, Hatzikiriakos S G, Englezos P. Physics of ice friction. *J Appl Phys* **107**(8): 081101 (2010)

[3] Nye J F. Glacier sliding without cavitation in a linear viscous approximation. *P Roy Soc A-Math Phy* **315**(1522): 381–403 (1970)

[4] Persson B N J. Ice friction: Glacier sliding on hard randomly rough bed surface. *J Chem Phys* **149**(23): 234701 (2018)

[5] Bäurle L, Kaempfer T U, Szabó D, Spencer N D. Sliding friction of polyethylene on snow and ice: Contact area and modeling. *Cold Reg Sci Technol* **47**(3): 276–289 (2007)

[6] Faraday M. On regelation, and on the conservation of force. *Lond Edinb Dublin Philos Mag J Sci* **17**(113): 162–169 (1859)

[7] Demmenie M, Kolpakov P, Nagata Y, Woutersen S, Bonn D. Scratch-healing behavior of ice by local sublimation and condensation. *J Phys Chem C* **126**(4): 2179–2183 (2022)

[8] Thomson J. I. On recent theories and experiments regarding ice at or near its melting-point. *P Roy Soc A-Math Phy* **10**: 151–160 (1859)

[9] Bowden F P, Hughes T P. The mechanism of sliding on ice and snow. *P Roy Soc A-Math Phy* **172**(949): 280–298 (1939)

[10] Frenken J W M, van der Veen J F. Observation of surface melting. *Phys Rev Lett* **54**(2): 134–137 (1985)

[11] Slater B, Michaelides A. Surface premelting of water ice. *Nat Rev Chem* **3**(3): 172–188 (2019)

[12] Lipowsky R. Critical surface phenomena at first-order bulk transitions. *Phys Rev Lett* **49**(21): 1575–1578 (1982)

[13] Tartaglino U, Zykova-Timan T, Ercolessi F, Tosatti E. Melting and nonmelting of solid surfaces and nanosystems. *Phys Rep* **411**(5): 291–321 (2005)

[14] Limmer D T. Closer look at the surface of ice. *PNAS* **113**(14): 12347–12349 (2016)

[15] Qiu Y Q, Molinero V. Why is it so difficult to identify the onset of ice premelting? *J Phys Chem Lett* **9**(17): 5179–5182 (2018)

[16] Li Y M, Somorjai G A. Surface premelting of ice. *J Phys Chem C* **111**(27): 9631–9637 (2007)

[17] Orndorf N, Singla S, Dhinojwala A. Transition in the acid–base component of surface free energy of ice upon the premelting of its second molecular bilayer. *J Phys Chem C* **124**(36): 19588–19594 (2020)

[18] Baran L, Llombart P, Rzysko W, MacDowell L G. Ice friction at the nanoscale. https://doi.org/10.48550/arXiv.2206.01313 (2022)

[19] Thomson E S, Hansen-Goos H, Wettlaufer J S, Wilen L A.

Grain boundary melting in ice. *J Chem Phys* **138**(12): 124707 (2013)
[20] Torabi Rad M, Boussinot G, Apel M. Dynamics of grain boundary premelting. *Sci Rep* **10**: 21074 (2020)
[21] Liefferink R W, Hsia F C, Weber B, Bonn D. Friction on ice: How temperature, pressure, and speed control the slipperiness of ice. *Phys Rev X* **11**: 011025 (2021)
[22] Canale L, Comtet J, Niguès A, Cohen C, Clanet C, Siria A, Bocquet L. Nanorheology of interfacial water during ice gliding. *Phys Rev X* **9**(4): 041025 (2019)
[23] Van Dongen M E H, Smeulders D M J. Ice speed skating: Onset of lubrication by frictional heating. *Europhys Lett* **134**(3): 34005 (2021)
[24] Roberts A D. Rubber–ice adhesion and friction. *J Adhesion* **13**(1): 77–86 (1981)
[25] Roberts A D, Richardson J C. Interface study of rubber–ice friction. *Wear* **67**(1): 55–69 (1981)
[26] Higgins D D, Marmo B A, Jeffree C E, Koutsos V, Blackford J R. Morphology of ice wear from rubber–ice friction tests and its dependence on temperature and sliding velocity. *Wear* **265**(5–6): 634–644 (2008)
[27] Lahayne O, Pichler B, Reihsner R, Eberhardsteiner J, Suh J, Kim D, Nam S, Paek H, Lorenz B, Persson B N J. Rubber friction on ice: Experiments and modeling. *Tribol Lett* **62**(2): 17 (2016)
[28] Tuononen A J, Kriston A, Persson B N J. Multiscale physics of rubber–ice friction. *J Chem Phys* **145**(11): 114703 (2016)
[29] Klapproth C, Kessel T M, Wiese K, Wies B. An advanced viscous model for rubber–ice-friction. *Tribol Int* **99**: 169–181 (2016)
[30] Scaraggi M, Persson B N J. Friction and universal contact area law for randomly rough viscoelastic contacts. *J Phys Condens Matter* **27**(10): 105102 (2015)
[31] Sukhomlinov S, Müser M H. On the viscous dissipation caused by randomly rough indenters in smooth sliding motion. *Appl Surf Sci Adv* **6**: 100182 (2021)
[32] Persson B N J. Theory of rubber friction and contact mechanics. *J Chem Phys* **115**(8): 3840–3861 (2001)
[33] Kennedy F E, Schulson E M, Jones D E. The friction of ice on ice at low sliding velocities. *Philos Mag A* **80**(5): 1093–1110 (2000)
[34] Persson B N J. Ice friction: Role of non-uniform frictional heating and ice premelting. *J Chem Phys* **143**(22): 224701 (2015)
[35] Hemette S, Cayer-Barrioz J, Mazuyer D. Thermal effects versus viscoelasticity in ice–rubber friction mechanisms. *Tribol Int* **162**: 107129 (2021)
[36] Bowden F P. Friction on snow and ice. *P Roy Soc A-Math Phy* **217**(1131): 462–478 (1953)
[37] Almqvist A, Pellegrini B, Lintzén N, Emami N, Holmberg H C, Larsson R. A scientific perspective on reducing ski–snow friction to improve performance in Olympic cross-country skiing, the biathlon and Nordic combined. *Frontiers in Sports and Active Living* **4**: 844883 (2022)
[38] Kalliorinne K, Sandberg J, Hinder G, Larsson R, Holmberg H C, Almqvist A. Snow contact characterisation of cross-country skis: A macro-scale study of the apparent contact. https://www.preprints.org/manuscript/202208.0512/v1 (2022)
[39] Butler M D, Vella D. Liquid bridge splitting enhances normal capillary adhesion and resistance to shear on rough surfaces. *J Colloid Interf Sci* **607**: 514–529 (2022)
[40] Koenen A, Sanon A. Tribological and vibroacoustic behavior of a contact between rubber and glass (application to wiper blade). *Tribol Int* **40**(10–12): 1484–1491 (2007)
[41] Persson B N J, Scaraggi M. On the transition from boundary lubrication to hydrodynamic lubrication in soft contacts. *J Phys Condens Matter* **21**(18): 185002 (2009)
[42] Deleau F, Mazuyer D, Koenen A. Sliding friction at elastomer/glass contact: Influence of the wetting conditions and instability analysis. *Tribol Int* **42**(1): 149–159 (2009)
[43] Persson B N J. Capillary adhesion between elastic solids with randomly rough surfaces. *J Phys Condens Matter* **20**(31): 315007 (2008)
[44] Gao T Y, Ye J X, Zhang K S, Liu X J, Zhang Y, Liu K. Role of capillary adhesion in the friction peak during the tacky transition. *Friction* **10**(8): 1208–1216 (2022)
[45] Lorenz B, Rodriguez N, Mangiagalli P, Persson B N J. Role of hydrophobicity on interfacial fluid flow: Theory and some applications. *Eur Phys J E* **37**(6): 57 (2014)
[46] Kawasaki S, Tada T, Persson B N J. Adhesion and friction between glass and rubber in the dry state and in water: Role of contact hydrophobicity. *Soft Matter* **14**(26): 5428–5441 (2018)

Toshio TADA. He is a general manager working for Sumitomo Rubber industries, Ltd. in Japan. His original field of expertise is polymer rheology and polymer physics. His expertise covers friction, wear, fracture, and continuum mechanics of elastomers, based on experience of manager of material testing for over 15 years. He received his Ph.D. degree of engineering of Kyoto university, Japan, in 1998.

Satoshi KAWASAKI. He received his M.S. degree of engineering of Osaka university, Japan, in 2005. He has been working for Sumitomo Rubber Industries, Ltd. in Japan since 2005. He is a manager responsible for friction mechanics of rubber.

Ryouske SHIMIZU. He received his M.S. degree of engineering of Kyoto university, Japan, in 2018. He has been working for Sumitomo Rubber Industries, Ltd. In Japan since 2018. He is responsible for friction mechanics of rubber, especially on ice.

Bo N. J. PERSSON. He is a research scientist at the Research Center Jülich, and CEO of Multiscale Consulting, a company specialized on consulting about contact mechanics problems like rubber friction, adhesion and leakage of seals. He got his Ph.D. degree in "*Dynamical Processes at Surfaces*" in 1980 but has worked on tribology problems since 1994. He is the author of "*Sliding Friction: Physical Principles and Applications*" (Springer, 1998, 2000) and coauthor with Prof. VOLOKITIN on "*Electromagnetic Fluctuations at the Nanoscale*" (Springer, 2017).